

G.F. Burgio · M. Baldo · O.E. Nicotra · H.-J. Schulze

A microscopic equation of state for protoneutron stars

Received: date / Accepted: date

Abstract We study the structure of protoneutron stars within the finite-temperature Brueckner-Bethe-Goldstone many-body theory. If nucleons, hyperons, and leptons are present in the stellar core, we find that neutrino trapping stiffens considerably the equation of state, because hyperon onsets are shifted to larger baryon density. However, the value of the critical mass turns out to be smaller than the “canonical” value $1.44 M_{\odot}$. We find that the inclusion of a hadron-quark phase transition increases the critical mass and stabilizes it at about $1.5\text{--}1.6 M_{\odot}$.

Keywords Dense matter · Equation of State · Neutron Stars

PACS 26.60.+c · 21.65.+f · 24.10.Cn · 97.60.Jd

1 Introduction

After a protoneutron star (PNS) is successfully formed in a supernova explosion, neutrinos are temporarily trapped within the star (Prakash et al. 1997). The subsequent evolution of the PNS is strongly dependent on the stellar composition, which is mainly determined by the number of trapped neutrinos, and by thermal effects with values of temperatures up to $30\text{--}40$ MeV (Burrows and Lattimer 1986; Pons et al. 1999). Hence, the equation of state (EOS) of dense matter at finite temperature is crucial for studying the macrophysical evolution of PNS.

Talk given by G.F. Burgio

G.F. Burgio
INFN Sezione di Catania, Via S. Sofia 64, I-95123 Catania, Italy
E-mail: fiorella.burgio@ct.infn.it

M. Baldo
INFN Sezione di Catania, Via S. Sofia 64, I-95123 Catania, Italy

O.E. Nicotra
INFN Sezione di Catania, Via S. Sofia 64, I-95123 Catania, Italy

H.-J. Schulze
INFN Sezione di Catania, Via S. Sofia 64, I-95123 Catania, Italy

Only a few microscopic calculations of the nuclear EOS at finite temperature are available so far. The variational calculation by Friedman and Pandharipande (1981) was one of the first semi-microscopic investigations of the finite-temperature EOS. The results predict a Van der Waals behavior for symmetric matter, which leads to a liquid-gas phase transition with a critical temperature $T_c \approx 18\text{--}20$ MeV. Later, Brueckner calculations (Lejeune et al. 1986; Baldo and Ferreira 1999) and chiral perturbation theory at finite temperature (Kaiser et al. 2002) confirmed these findings with very similar values of T_c . The Van der Waals behavior was also found in the finite-temperature relativistic Dirac-Brueckner calculations of Ter Haar and Malfliet (1986, 1987) and Huber et al. (1999), although at a lower temperature.

We have developed a microscopic EOS in the framework of the Brueckner-Bethe-Goldstone (BBG) many-body approach including nucleons and hyperons and extended to finite temperature. This EOS has been successfully applied to the study of the limiting temperature in nuclei (Baldo et al. 1999, 2004). Recently, this EOS has been extended for including neutrino trapping, and results have been presented in Nicotra et al. (2006a).

The scope of this work is to discuss composition and structure of these newly born stars with the EOS previously mentioned, also including a possible transition to quark matter. In fact, superdense matter in PNS cores may consist of weakly interacting quarks rather than hadrons, due to the asymptotic freedom. The appearance of quarks can alter substantially the chemical composition of a PNS, with observable consequences on the evolution, like onset of metastability and abrupt cessation of the neutrino signal (Pons et al. 2001).

We have studied the effects of a hadron-quark phase transition within the MIT bag model, and found that the presence of quark matter increases the value of the maximum mass of a PNS, and stabilizes it at about $1.5\text{--}1.6 M_{\odot}$, no matter the value of the temperature.

This paper is organized as follows. In Sec. 2 we briefly review the BBG theory of nuclear matter at finite temperature, including both nucleons and hyperons. In Sec. 3 we discuss the chemical composition of a PNS, whereas in Sec. 4

we study its structure, even including a possible transition to a quark phase. Finally, in Sec. 5, we draw our conclusions.

2 The BBG EOS at finite temperature

In the recent years, the BBG perturbative theory has made much progress, since its convergence has been firmly established (Day 1981; Song et al. 1998; Baldo et al. 2000b; Sartor 2006), and has been extended in a fully microscopic and self-consistent way to the hyperonic sector (Schulze et al. 1995, 1998, 2006; Baldo et al. 1998, 2000a). Moreover, the addition of phenomenological three-body forces (TBF) based on the Urbana model (Carlson et al. 1983; Schiavilla et al. 1986), permitted to improve to a large extent the agreement with the empirical saturation properties (Baldo et al. 1997; Zhou et al. 2004).

The finite-temperature formalism which is closest to the BBG expansion, and actually reduces to it in the zero-temperature limit, is the one formulated by Bloch and De Dominicis (1958, 1959). In this approach the essential ingredient is the two-body scattering matrix K , which, along with the single-particle potential U , satisfies the self-consistent equations

$$\begin{aligned} \langle k_1 k_2 | K(W) | k_3 k_4 \rangle &= \langle k_1 k_2 | V | k_3 k_4 \rangle \\ &+ \text{Re} \sum_{k'_3 k'_4} \langle k_1 k_2 | V | k'_3 k'_4 \rangle \frac{[1 - n(k'_3)][1 - n(k'_4)]}{W - E_{k'_3} - E_{k'_4} + i\epsilon} \langle k'_3 k'_4 | K(W) | k_3 k_4 \rangle \end{aligned} \quad (1)$$

and

$$U(k_1) = \sum_{k_2} n(k_2) \langle k_1 k_2 | K(W) | k_1 k_2 \rangle_A, \quad (2)$$

where k_i generally denote momentum, spin, and isospin. Here V is the two-body interaction, and we choose the Argonne V_{18} nucleon-nucleon potential (Wiringa et al. 1995). $W = E_{k_1} + E_{k_2}$ represents the starting energy, and $E_k = k^2/2m + U(k)$ the single-particle energy. Eq. (1) coincides with the Brueckner equation for the K matrix at zero temperature, if the single-particle occupation numbers $n(k)$ are taken at $T = 0$. At finite temperature $n(k)$ is a Fermi distribution. For a given density and temperature, Eqs. (1) and (2) have to be solved self-consistently along with the equation for the grand-canonical potential density ω and the free energy density, which has the following simplified expression

$$f = \sum_i \left[\sum_k n_i(k) \left(\frac{k^2}{2m_i} + \frac{1}{2} U_i(k) \right) - T s_i \right], \quad (3)$$

where

$$s_i = - \sum_k \left(n_i(k) \ln n_i(k) + [1 - n_i(k)] \ln [1 - n_i(k)] \right) \quad (4)$$

is the entropy density for component i treated as a free gas with spectrum $E_i(k)$. For a more extensive discussion of this topic, the reader is referred to (Baldo 1999) and references therein.

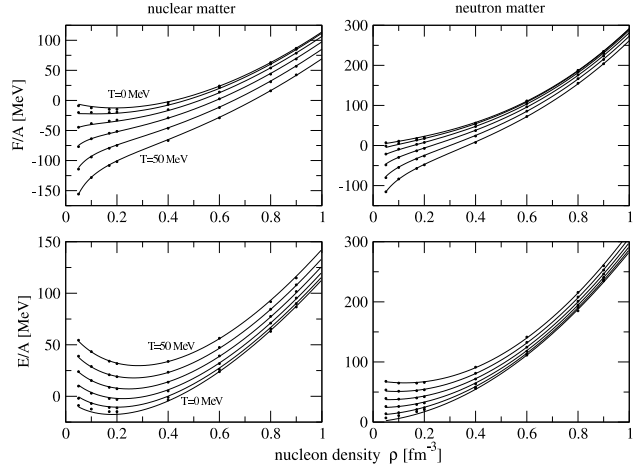


Fig. 1 Finite-temperature BBG EOS for symmetric (left-hand panels) and purely neutron (right-hand panels) matter. The upper panels show the free energy and the lower panels the internal energy per particle as a function of the nucleon density. The temperatures vary from 0 to 50 MeV in steps of 10 MeV.

In deriving Eq. (3), we have introduced the so-called *Frozen Correlations Approximation*, i.e., the correlations at $T \neq 0$ are assumed to be essentially the same as at $T = 0$. This means that the single-particle potential $U_i(k)$ for the component i can be approximated by the one calculated at $T = 0$. This allows to save computational time and simplify the numerical procedure. It turns out that the assumed independence is valid to a good accuracy, at least for not too high temperature (Baldo and Ferreira 1999, Fig. 12).

In our many-body approach, we have also introduced TBF among nucleons, in order to reproduce correctly the nuclear matter saturation point $\rho_0 \approx 0.17 \text{ fm}^{-3}$, $E/A \approx -16 \text{ MeV}$. Since a complete microscopic theory of TBF is not available yet, we have adopted the phenomenological Urbana model (Carlson et al. 1983; Schiavilla et al. 1986), which consists of an attractive term due to two-pion exchange with excitation of an intermediate Δ resonance, and a repulsive phenomenological central term. In the BBG approach, the TBF is reduced to a density-dependent two-body force by averaging over the position of the third particle, assuming that the probability of having two particles at a given distance is reduced according to the two-body correlation function. The corresponding EOS reproduces correctly the nuclear matter saturation point (Baldo et al. 1997; Zhou et al. 2004), and gives values of incompressibility and symmetry energy at saturation compatible with those extracted from phenomenology (Myers and Swiatecki 1996).

In Fig. 1 we display the free energy (upper panels) and the internal energy (lower panels) obtained following the above discussed procedure, both for symmetric and purely neutron matter, as a function of the nucleon density. Calculations are reported for several values of the temperature be-

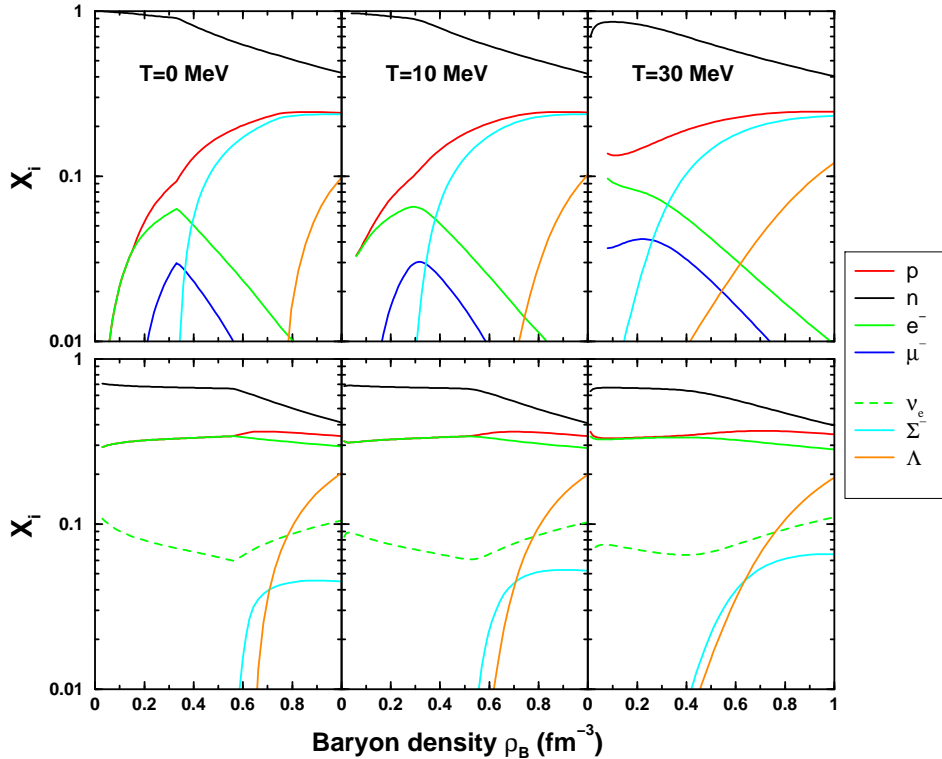


Fig. 2 Relative populations for neutrino-free (upper panels) and neutrino-trapped (lower panels) matter as a function of the baryon density for several values of the temperature.

tween 0 and 50 MeV. We notice that the free energy of symmetric matter shows a typical Van der Waals behavior (with $T_c \approx 16$ MeV) and is a monotonically decreasing function of the temperature. On the contrary, the internal energy is an increasing function of the temperature. At $T = 0$ the free energy coincides with the total energy and the corresponding curve is just the usual nuclear matter saturation curve.

2.1 Inclusion of hyperons

The fast rise of the baryon chemical potentials with density in neutron star cores (Glendenning 1982, 1985) may trigger the appearance of strange baryonic species, i.e., hyperons. For this purpose we have extended the BBG approach in order to include the Σ^- and Λ hyperons (Schulze et al. 1998, 2006; Baldo et al. 1998, 2000a). The inclusion of hyperons requires the knowledge of the nucleon-hyperon (NH) and hyperon-hyperon (HH) interactions. In our past papers, we have shown results obtained at $T = 0$, and we have used the Nijmegen soft-core NH potential (Maessen et al. 1989), and neglected the HH interactions, since no reliable HH potentials are available yet. For these reasons, we present in this article finite-temperature calculations using free hyperons. A more complete set of calculations obtained with the inclusion of the NH interaction at finite temperature will be published elsewhere.

We have found that due to its negative charge the Σ^- hyperon is the first strange baryon appearing in the reaction $n + n \rightarrow p + \Sigma^-$, in spite of its substantially larger mass compared to the neutral Λ hyperon ($M_{\Sigma^-} = 1197$ MeV, $M_{\Lambda} = 1116$ MeV). The presence of hyperons strongly softens the EOS, mainly due to the larger number of baryonic degrees of freedom. This EOS produces a maximum neutron star mass that lies slightly below the canonical value of $1.44 M_{\odot}$ (Taylor and Weisberg 1989), as confirmed by Schulze et al. (2006) also with the NSC97 hyperon potentials (Stoks and Rijken 1999). This could indicate the presence of non-baryonic (quark) matter in the interior of heavy neutron stars (Burgio et al. 2002a, 2002b; Baldo et al. 2003; Maieron et al. 2004). This point is discussed more extensively below.

3 Composition and EOS of hot stellar matter

For stars in which the strongly interacting particles are only baryons, the composition is determined by the requirements of charge neutrality and equilibrium under the weak processes

$$B_1 \rightarrow B_2 + l + \bar{\nu}_l, \quad B_2 + l \rightarrow B_1 + \nu_l, \quad (5)$$

where B_1 and B_2 are baryons and l is a lepton, either an electron or a muon. When the neutrinos are trapped, these two requirements imply that the relations

$$\sum_i q_i x_i + \sum_l q_l x_l = 0 \quad (6)$$

and

$$\mu_i = b_i \mu_n - q_i (\mu_l - \mu_{\nu_l}) \quad (7)$$

are satisfied. In the expression above, $x_i = \rho_i / \rho_B$ represents the baryon fraction for the species i , μ_i the chemical potential, b_i the baryon number, and q_i the electric charge. Equivalent quantities are defined for the leptons l .

For stellar matter containing nucleons and hyperons as relevant degrees of freedom, the chemical equilibrium conditions read explicitly

$$\begin{aligned} \mu_n - \mu_p &= \mu_e - \mu_{\nu_e} = \mu_\mu + \mu_{\bar{\nu}_\mu}, \\ \mu_{\Sigma^-} &= 2\mu_n - \mu_p, \\ \mu_\Lambda &= \mu_n. \end{aligned} \quad (8)$$

The nucleon chemical potentials are calculated starting from the free energy and its partial derivatives with respect to the total baryon density ρ and proton fraction x_p , i.e.,

$$\mu_n(\rho, x_p) = \left[1 + \rho \frac{\partial}{\partial \rho} - x_p \frac{\partial}{\partial x_p} \right] \frac{f}{\rho}, \quad (9)$$

$$\mu_p(\rho, x_p) = \left[1 + \rho \frac{\partial}{\partial \rho} + (1 - x_p) \frac{\partial}{\partial x_p} \right] \frac{f}{\rho}, \quad (10)$$

whereas the chemical potentials of the noninteracting leptons and hyperons are obtained by solving numerically the free Fermi gas model at finite temperature. More details are given in Nicotra et al. (2006a).

Because of trapping, the numbers of leptons per baryon of each flavor $l = e, \mu$,

$$Y_l = x_l - x_{\bar{l}} + x_{\nu_l} - x_{\bar{\nu}_l}, \quad (11)$$

are conserved on dynamical time scales. Gravitational collapse calculations of the white-dwarf core of massive stars indicate that at the onset of trapping, the electron lepton number $Y_e = x_e + x_{\nu_e} \approx 0.4$, the precise value depending on the efficiency of electron capture reactions during the initial collapse stage. Moreover, since no muons are present when neutrinos become trapped, the constraint $Y_\mu = x_\mu - x_{\bar{\nu}_\mu} = 0$ can be imposed. We fix the Y_l at these values in our calculations for neutrino-trapped matter.

Let us now discuss first the populations of beta-equilibrated stellar matter, by solving the chemical equilibrium conditions given by Eqs. (8), supplemented by electrical charge neutrality and baryon number conservation. In Fig. 2 we show the particle fractions as a function of baryon density, for different values of the temperature. The upper panels show the particle fractions when stellar matter does not contain neutrinos, whereas the lower panels show the populations in neutrino-trapped matter. We observe that the electron fraction is larger in neutrino-trapped than in neutrino-free matter, and, as a consequence, the proton population is larger.

Neutrino trapping strongly influences the onset of hyperons. In fact, the threshold density of the Σ^- is shifted to high density, whereas Λ 's appear at slightly smaller density. This is due to the fact that the Σ^- onset depends on the neutron and lepton chemical potentials, i.e., $\mu_n + \mu_e -$

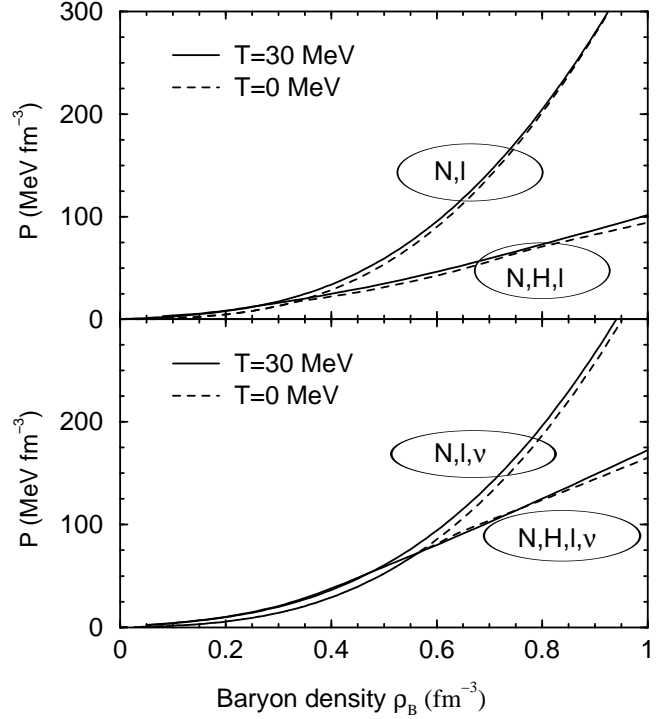


Fig. 3 Pressure as a function of baryon density for beta-equilibrated matter at temperatures $T = 0$ and 30 MeV. The upper (lower) panel shows the EOS in neutrino-free (neutrino-trapped) matter, with nucleons only (upper curves) and nucleons plus hyperons (lower curves).

μ_{ν_e} , which stays at larger values in neutrino-trapped matter than in the neutrino-free case because of the larger fraction of electrons, thus delaying the appearance of the Σ^- to higher baryon density and limiting its population to a few percent. On the other hand, the Λ onset depends on the neutron chemical potential only, which keeps at lower values in the neutrino-trapped case. When the temperature increases, more and more hyperons are present also at low densities, but they represent only a small fraction of the total baryon density in this region of the PNS. Altogether, the hyperon fractions are much smaller than in the neutrino-free matter. Therefore the corresponding EOS will be stiffer than in the neutrino-free case.

Once the composition of the β -stable stellar matter is known, one can proceed to calculate the free energy density f and then the pressure p through the usual thermodynamical relation

$$p = \rho^2 \frac{\partial(f/\rho)}{\partial \rho}. \quad (12)$$

The resulting EOS is displayed in Fig. 3, where the pressure for beta-stable asymmetric matter, without (upper panel) and with (lower panel) neutrinos, is plotted as a function of the baryon density at temperatures $T = 0$ and 30 MeV. Let us begin with discussing the case of neutrino-free matter, shown without (upper curves) and with hyperons (lower curves). We notice that thermal effects produce a slightly stiffer EOS with respect to the cold case, and that at very high densities they almost play no role.

In the case that only nucleons are present, the EOS gets softer with increasing temperature at high baryon density. This behavior is at variance with the results obtained by Prakash et al. (1997). In this regard, we should notice that in our calculations we are considering an isothermal profile, whereas in Prakash et al. (1997) the profile is isentropic. Another difference between the two approaches is in the many-body method. A complete comparison can be made only by adopting an isentropic description within our BHF approach. This matter is left to further investigations.

The inclusion of hyperons produces a dramatic effect, because the EOS gets much softer, no matter the value of the temperature. In this case, thermal effects dominate over the whole density range since on the average the Fermi energies are smaller. A similar behavior was found in Prakash et al. (1997).

In the lower panel we show the corresponding neutrino-trapped case. The EOS is slightly softer than in the neutrino-free case if only nucleons and leptons are present in the stellar matter. Again, the presence of hyperons introduces a strong softening of the EOS, but less than in the neutrino-free case, because now the hyperons appear later in the matter and their concentration is lower. Thermal effects are rather small also in this case, except for the disappearance of the hyperon onsets.

4 (Proto)neutron star structure

The stable configurations of a (proto)neutron star can be obtained from the well-known hydrostatic equilibrium equations of Tolman, Oppenheimer, and Volkov (Shapiro and Teukolsky 1983) for the pressure p and the enclosed mass m ,

$$\frac{dp(r)}{dr} = -\frac{Gm(r)\varepsilon(r)}{r^2} \frac{\left[1 + \frac{p(r)}{\varepsilon(r)}\right] \left[1 + \frac{4\pi r^3 p(r)}{m(r)}\right]}{1 - \frac{2Gm(r)}{r}}, \quad (13)$$

$$\frac{dm(r)}{dr} = 4\pi r^2 \varepsilon(r), \quad (14)$$

once the EOS $p(\varepsilon)$ is specified, being ε the total energy density (G is the gravitational constant). For a chosen central value of the energy density, the numerical integration of Eqs. (13) and (14) provides the mass-radius relation.

For the description of the (proto)neutron star crust, we have joined the hadronic EOS described above with the ones by Negele and Vautherin (1973) in the medium-density regime ($0.001 \text{ fm}^{-3} < \rho < 0.08 \text{ fm}^{-3}$), and the ones by Feynman, Metropolis, and Teller (1949) and Baym, Pethick, and Sutherland (1971) for the outer crust ($\rho < 0.001 \text{ fm}^{-3}$).

Simulations of supernovae explosions (Burrows and Latimer 1986; Pons 1999) show that the PNS has neither an isentropic nor an isothermal profile. For simplicity we will assume a constant temperature inside the star and attach a cold crust for the outer part. This schematizes the temperature profile of the PNS. More realistic temperature profiles can be obtained by modelling the neutrinosphere both

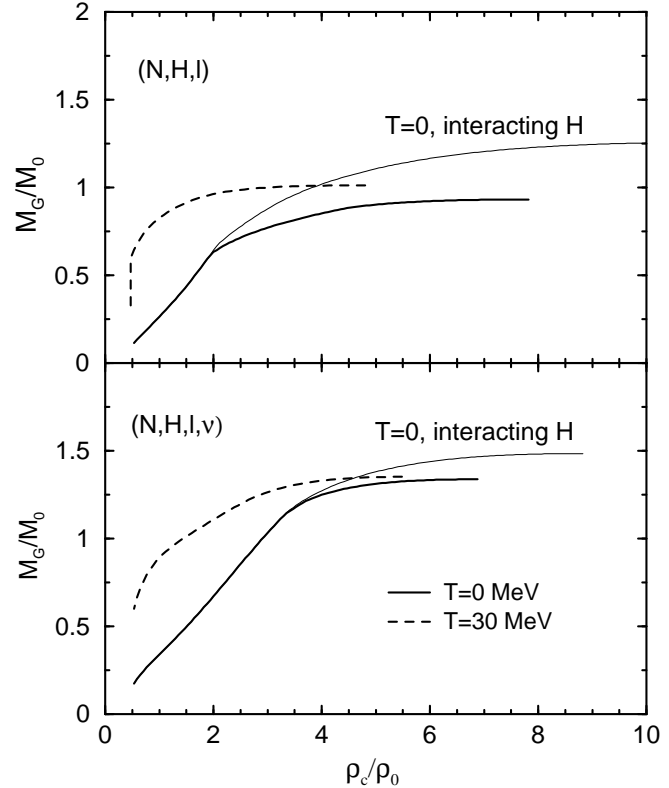


Fig. 4 The gravitational mass (in units of the solar mass) as a function of the central baryon density (normalized with respect to the saturation value $\rho_0 = 0.17 \text{ fm}^{-3}$) at temperatures $T = 0$ and 30 MeV . The upper (lower) plot regards neutrino-free (neutrino-trapped) matter. The thin solid curves denote configurations of cold stars employing interacting hyperons, whereas the remaining curves show results obtained using free hyperons.

in the interior and in the external outer envelope, which is expected to be much cooler. A proper treatment of the transition from the hot interior to the cold outer part can have a dramatic influence on the mass-central density relation in the region of low central density and low stellar masses. In particular, the “minimal mass” region, typical of cold neutron stars (Zel’dovich and Novikov 1971; Shapiro and Teukolsky 1983), can be shifted in PNS to much higher values of central density and masses. A detailed analysis of this point can be found in (Gondek et al. 1997), where a model of the transition region between the interior and the external envelope is developed. However, as discussed in the next section, the maximum mass region is not affected by the structure of this low-density transition region.

In Fig. 4 we show the gravitational mass (in units of the solar mass $M_\odot = 1.98 \times 10^{33} \text{ g}$) as a function of the central baryon density for stars containing hyperons. We observed in Fig. 3 that the EOS softens considerably when hyperons are included, both in neutrino-free and neutrino-trapped matter. As a consequence the mass – central density relation is also significantly altered by the presence of hyperons and the value of the critical mass is about $1.3 M_\odot$ for neutron

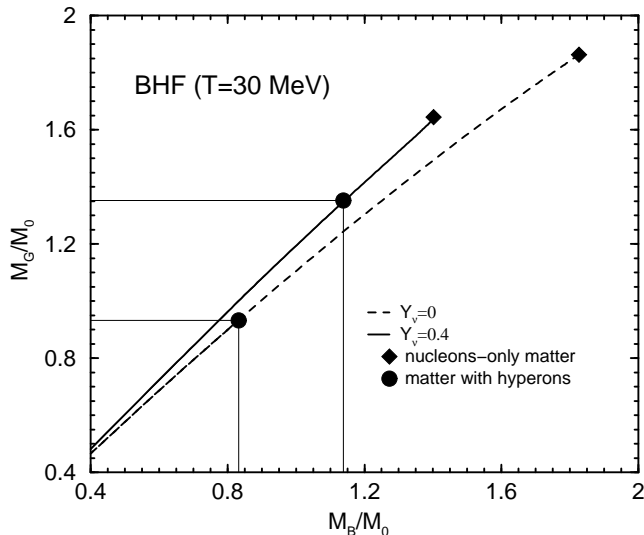


Fig. 5 Gravitational mass as a function of the baryon mass for neutrino-trapped matter at temperature $T = 30$ MeV (solid curve) and for cold neutrino-free matter (dashed curve). A dot at the end of the curves indicates matter with noninteracting hyperons, a diamond indicates purely nucleonic matter.

stars (upper plot, thin curve) and $1.5 M_{\odot}$ for protostars in the ν -trapped stage (lower plot, thin curve). Those results are obtained employing interacting hyperons at zero temperature, choosing the Nijmegen potential as nucleon-hyperon potential (Maessen et al. 1989), which is well adapted to the available experimental NH scattering data. However, since the value of the critical mass for cold stars falls below the mass of the best observed pulsar, i.e., $1.44 M_{\odot}$ (Taylor and Weisberg 1989), the EOS of high-density nuclear matter comprising only baryons (nucleons and hyperons) is probably unrealistic (even taking into account the present uncertainty of hyperonic two-body and three-body forces), and must be supplemented by a transition to quark matter. This has been discussed extensively in (Burgio et al. 2002a, 2002b; Baldo et al. 2003; Maieron et al. 2004), and will be briefly recalled in the next subsection.

Nevertheless, it is interesting to observe that the maximum mass of hyperonic protostars is larger (by about $0.3 M_{\odot}$) than the one of cold neutron stars. The reason is the minor importance of hyperons in the neutrino-saturated matter, which leads to a stiffer EOS, see Fig. 3, and to a larger maximum mass. This feature could lead to metastable stars suffering a delayed collapse while cooling down, as discussed in (Prakash et al. 1997; Pons et al. 1999). Metastable stars occur within a range of masses near the maximum mass of the initial configuration and remain stable only for several seconds after formation. In order to study metastability, it is useful to calculate the baryonic mass M_B , which is proportional to the number of baryons in the system and is constant during the evolution of the isolated star, if no accretion is as-

sumed during the entire PNS evolution. For that, Eqs. (13) and (14) must be supplemented with

$$\frac{dM_B(r)}{dr} = \frac{4\pi r^2 \rho_B m_N}{\sqrt{1 - 2Gm(r)/r}}, \quad (15)$$

where $m_N = 1.67 \times 10^{-24}$ g is the nucleon mass. As one can see from Fig. 5, if hyperons are present (lines ending with a dot), then deleptonization, that is the transition from $Y_{\nu} = 0.4$ to $Y_{\nu} = 0$, lowers the range of baryonic masses that can be supported by the EOS from about $1.15 M_{\odot}$ to about $0.84 M_{\odot}$. The window in the baryonic mass in which neutron stars are metastable is thus about $0.31 M_{\odot}$. On the other hand, if hyperons are absent (lines ending with a diamond), the maximum baryonic mass increases during deleptonization, and no metastability occurs.

4.1 Including quark matter

The appearance of quark matter in the interior of massive neutron stars is one of the main issues in the physics of these compact objects. Calculations of neutron star structure, based on microscopic nucleonic EOS, indicate that the central particle density may reach values larger than $1/\text{fm}^3$. In this density range the nucleon cores (dimension ≈ 0.5 fm) start to touch each other, and it is hard to imagine that only nucleonic degrees of freedom can play a role. Rather, it can be expected that even before reaching these density values, the nucleons start to lose their identity, and quark degrees of freedom are excited at a macroscopic level. Unfortunately, while the microscopic theory of the nucleonic EOS has reached a high degree of sophistication, the quark matter EOS is poorly known at zero temperature and at the high baryonic density appropriate for NS.

Here we will briefly discuss some results obtained by using the MIT bag model (Chodos et al. 1974) at finite temperature, with a bag constant $B = 90 \text{ MeVfm}^{-3}$. In order to study the hadron-quark phase transition, we have performed a Maxwell construction between the baryon phase and the quark phase. A more realistic model is the Glendenning construction (Glendenning 1992), which determines the range of baryon density where both phases coexist, yielding an EOS containing a pure hadronic phase, a mixed phase, and a pure quark matter region. Using the Maxwell construction implies that the phase transition is sharp, and no mixed phase exists. The pressure is characterized by a plateau extended over a range of baryon density, which separates the purely hadron phase at low density from the pure quark phase at higher density.

This is shown in Fig. 6, which displays the case of hot, neutrino-trapped matter. The solid line represents the EOS with the hadron-quark phase transition, whereas the dashed line is the purely hadronic case. As we can see, the EOS which comprises the hadron and the quark phases is stiffer at large baryon density than the purely hadronic case. A stiffer EOS causes larger values of the critical mass for a neutron star, as we found in (Burgio et al. 2002b).

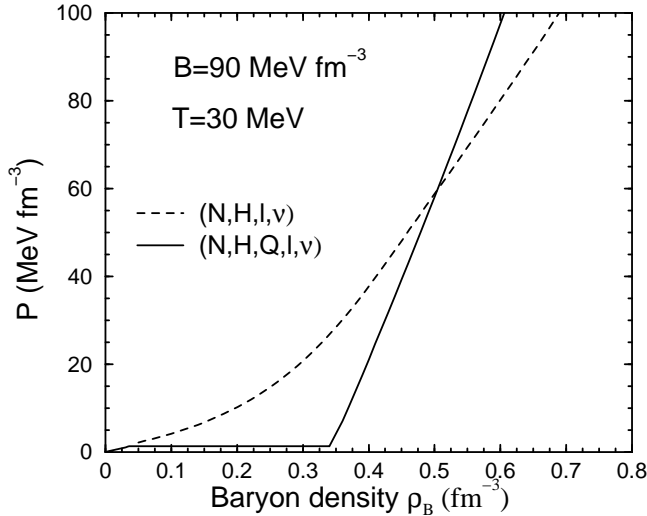


Fig. 6 Pressure as a function of the baryon density at temperature $T = 30$ MeV, and a bag constant $B = 90$ MeVfm $^{-3}$. The solid (dashed) curve is for neutrino-trapped matter containing baryons and quark matter (only baryons).

Table 1 The values of the maximum mass and corresponding central density (normalized with respect to the saturation density $\rho_0 = 0.17$ fm $^{-3}$) for different stellar configurations.

	T (MeV)	M_G/M_\odot	ρ_c/ρ_0
PNS	30	1.53	8.2
PNS	50	1.53	7.9
NS	0	1.5	9.5

In particular, the critical mass may reach values up to $1.5\text{--}1.6 M_\odot$, depending on the value of the bag constant. The maximum mass increases with decreasing value of B , but the latter cannot be too small if stability of symmetric nuclear matter at saturation has to be ensured. We have also checked that these results are quite general, and do not change appreciably if a density-dependent bag constant is introduced (Nicotra et al. 2006b).

In Table 1, we show the values of the critical mass for PNS with trapped neutrinos at temperatures $T=30$ and 50 MeV and compare with the value for a cold NS. We find that the hadron-quark phase transition stabilizes the value of the maximum mass, which turns out to be independent of the temperature and equal to $1.53 M_\odot$ for the adopted value of the bag constant. In this case we do not find any metastable stars, at variance with the findings of Prakash et al. (1997). More detailed calculations will be presented elsewhere (Nicotra et al. 2006b).

5 Conclusions

In this paper we have studied the structure of (proto)neutron stars on the basis of a microscopically derived EOS for baryonic matter at finite temperature, in the framework of

the Brueckner-Hartree-Fock many-body theory. Configurations with or without trapped neutrinos were considered. We found that the maximum mass of a hyperonic PNS is substantially larger than the one of the cold star, because both neutrino trapping and finite temperature tend to stiffen the EOS. Trapping shifts the onset of hyperons, in particular the Σ^- , to considerably higher density and reduces their concentrations.

However, as in the case of cold neutron stars, the addition of hyperons demands for the inclusion of quark degrees of freedom in order to obtain a maximum mass larger than the observational lower limit. For this purpose, we have studied the hadron-quark phase transition within the MIT bag model, and performed a Maxwell construction between the two phases. We found that the inclusion of quark matter stabilizes the value of the critical mass of a PNS at about $1.5\text{--}1.6 M_\odot$, no matter the value of the temperature.

References

- Baldo, M., Bombaci, I., Burgio, G.F.: A&A **328**, 274 (1997)
- Baldo, M., Burgio, G.F., Schulze, H.-J.: Phys. Rev. **C58**, 3688 (1998); **C61**, 055801 (2000a)
- Baldo, M.: Nuclear Methods and the Nuclear Equation of State, ed. World Scientific, Singapore, 1999
- Baldo, M., Ferreira, L.S.: Phys. Rev. **C59**, 682 (1999)
- Baldo, M., Song, H.Q., Giansiracusa, G., Lombardo, U.: Phys. Lett. **B473**, 1 (2000b)
- Baldo, M., Fiasconaro, A., Song, H.Q., Giansiracusa, G., Lombardo, U.: Phys. Rev. **C65**, 017303 (2001)
- Baldo, M., Buballa, M., Burgio, G.F., Neumann, F., Oertel, M., Schulze, H.-J.: Phys. Lett. **B562**, 153 (2003)
- Baldo, M., Ferreira, L.S., Nicotra, O.E.: Phys. Rev. **C69**, 034321 (2004)
- Baym, G., Pethick, C., Sutherland, D.: ApJ **170**, 299 (1971)
- Bloch, C., De Dominicis, C.: Nucl. Phys. **7**, 459 (1958); **10**, 181 (1959a); **10**, 509 (1959b)
- Burgio, G.F., Baldo, M., Sahu, P.K., Santra, A.B., Schulze, H.-J.: Phys. Lett. **B526**, 19 (2002a)
- Burgio, G.F., Baldo, M., Sahu, P.K., Schulze, H.-J.: Phys. Rev. **C66**, 025802 (2002b)
- Burrows, A., Lattimer, J.M.: ApJ 307, **178** (1986)
- Carlson, J., Pandharipande, V.R., Wiringa, R.B.: Nucl. Phys. **A401**, 59 (1983)
- Chodos, A., Jaffe, R.L., Johnson, K., Thorn, C.B., Weisskopf, V.F.: Phys. Rev. **D9**, 3471 (1974)
- Day, B.D.: Phys. Rev. **C24**, 1203 (1981)
- Feynman, R., Metropolis, F., Teller, E.: Phys. Rev. **75**, 1561 (1949)
- Friedman, B., Pandharipande, V.R.: Nucl. Phys. **A361**, 502 (1981)
- Glendenning, N.K.: Phys. Lett. **B114**, 391 (1982); ApJ **293**, 470 (1985); Phys. Rev. **D46**, 1274 (1992); Compact Stars, Nuclear Physics, Particle Physics, and General Relativity, 2nd ed., Springer-Verlag, New York, 2000
- Gondek, D., Haensel, P., Zdunik, J.L.: A&A **325**, 217 (1997)
- Huber, H., Weber, F., Weigel, M.K.: Phys. Rev. **C57**, 3484 (1999)
- Kaiser, N., Fritsch, S., Weise, W.: Nucl. Phys. **A697**, 255 (2002)
- Lejeune, A., Grangé, P., Martzloff, M., Cugnon, J.: Nucl. Phys. **A453**, 189 (1986)
- Maessen, P., Rijken, Th., de Swart, J.: Phys. Rev. **C40**, 2226 (1989)
- Maieron, C., Baldo, M., Burgio, G.F., Schulze, H.-J.: Phys. Rev. **D70**, 043010 (2004)
- Myers, W.D., Swiatecki, W.J.: Nucl. Phys. **A601**, 141 (1996)
- Negele, J.W., Vautherin, D.: Nucl. Phys. **A207**, 298 (1973)

28. Nicotra, O.E., Baldo, M., Burgio, G.F., Schulze, H.-J.: *A&A* **451**, 213 (2006a); e-print: astro-ph/0608021, submitted to PRD (2006b)
29. Pons, J.A., Reddy, S., Prakash, M., Lattimer, J.M., Miralles, J.A.: *ApJ* **513**, 780 (1999)
30. Pons, J.A., Steiner, A.W., Prakash, M., Lattimer, J.M.: *Phys. Rev. Lett.* **86**, 5223 (2001)
31. Prakash, M., Bombaci, I., Prakash, M., Ellis, P.J., Lattimer, J.M., Knorren, R.: *Phys. Rep.* **280**, 1 (1997)
32. Sartor, R.: *Phys. Rev.* **C73**, 034307 (2006)
33. Schiavilla, R., Pandharipande, V.R., Wiringa, R.B.: *Nucl. Phys.* **A449**, 219 (1986)
34. Schulze, H.-J., Lejeune, A., Cugnon, J., Baldo, M., Lombardo, U.: *Phys. Lett.* **B355**, 21 (1995)
35. Schulze, H.-J., Baldo, M., Lombardo, U., Cugnon, J., Lejeune, A.: *Phys. Rev.* **C57**, 704 (1998)
36. Schulze, H.-J., Polls, A., Ramos, A., Vidaña, I.: *Phys. Rev.* **C73**, 058801 (2006)
37. Shapiro, S.L., Teukolsky, S.A.: *Black Holes, White Dwarfs, and Neutron Stars*, John Wiley and Sons, New York, 1983
38. Song, H.Q., Baldo, M., Giansiracusa, G., Lombardo, U.: *Phys. Rev. Lett.* **81**, 1584 (1998)
39. Stoks, V.G.J., Rijken, Th.A.: *Phys. Rev.* **C59**, 3009 (1999)
40. Taylor, J.H., Weisberg, J.M.: *ApJ* **345**, 434 (1998)
41. Ter Haar, B., Malfliet, R.: *Phys. Rev. Lett.* **56**, 1237 (1986); *Phys. Rep.* **149**, 207 (1987)
42. Wiringa, R.B., Stoks, V.G.J., Schiavilla, R.: *Phys. Rev.* **C51**, 38 (1995)
43. Zel'dovich, Y.B., Novikov, I.D.: *Stars and Relativity*, The University of Chicago Press, Chicago, 1971
44. Zhou, X.R., Burgio, G.F., Lombardo, U., Schulze, H.-J., Zuo, W.: *Phys. Rev.* **C69**, 018801 (2004)